





Article

Non-Invasive Method to Predict the Composition of Requeijão Cremoso Directly in Commercial Packages Using Time Domain NMR Relaxometry and Chemometrics

Guilherme de Oliveira Machado ¹, Gustavo Galastri Teixeira ², Rodrigo Henrique dos Santos Garcia ¹ ,
Tiago Bueno Moraes ³ , Evandro Bona ⁴ , Poliana M. Santos ^{2,*} and Luiz Alberto Colnago ^{5,*} 

¹ Instituto de Química de São Carlos, Universidade de São Paulo, CP 369, São Carlos 13660-970, SP, Brazil; guilherme.oliveira.machado@usp.br (G.d.O.M.); rodrigogarciaquimico@yahoo.com.br (R.H.d.S.G.)

² Department of Microbiology, Institute of Biomedical Science, Universidade Tecnológica Federal do Paraná, Rua Deputado Heitor de Alencar Furtado, Curitiba 81280-340, PR, Brazil; gugalastri@hotmail.com

³ Depto. Engenharia de Biosistemas, Universidade de São Paulo, Av. Páduas Dias, Piracicaba 13418-900, SP, Brazil; tiagobuemoaraes@gmail.com

⁴ Programa de Pós-Graduação em Tecnologia de Alimentos (PPGTA), Universidade Tecnológica Federal do Paraná, Rua Rosalina Maria Ferreira, Campo Mourão 87301-899, PR, Brazil; ebona@utfpr.edu.br

⁵ Embrapa Instrumentação, Rua XV de Novembro, São Carlos 13560-970, SP, Brazil

* Correspondence: polianasantos@utfpr.edu.br (P.M.S.); luiz.colnago@embrapa.br (L.A.C.)

Abstract: Low Field Time-Domain Nuclear Magnetic Resonance (TD-NMR) relaxometry was used to determine moisture, fat, and defatted dry matter contents in “requeijão cremoso” (RC) processed cheese directly in commercial packaged (plastic cups or tubes with approximately 200 g). Forty-five samples of commercial RC types (traditional, light, lactose-free, vegan, and fiber) were analyzed using longitudinal (T_1) and transverse (T_2) relaxation measurements in a wide bore Halbach magnet (0.23 T) with a 100 mm probe. The T_1 and T_2 analyses were performed using CWFP- T_1 (Continuous Wave Free Precession) and CPMG (Carr-Purcell-Meiboom-Gill) single shot pulses. The scores of the principal component analysis (PCA) of CWFP- T_1 and CPMG signals did not show clustering related to the RC types. Optimization by variable selection was carried out with ordered predictors selection (OPS), providing simpler and predictive partial least squares (PLS) calibration models. The best results were obtained with CWFP- T_1 data, with root-mean-square errors of prediction (RMSEP) of 1.38, 4.71, 3.28, and 3.00% for defatted dry mass, fat in the dry and wet matter, and moisture, respectively. Therefore, CWFP- T_1 data modeled with chemometrics can be a fast method to monitor the quality of RC directly in commercial packages.

Keywords: TD-NMR; requeijão cremoso; CPMG; CWFP- T_1 ; PLS; OPS



Citation: de Oliveira Machado, G.; Teixeira, G.G.; Garcia, R.H.d.S.; Moraes, T.B.; Bona, E.; Santos, P.M.; Colnago, L.A. Non-Invasive Method to Predict the Composition of Requeijão Cremoso Directly in Commercial Packages Using Time Domain NMR Relaxometry and Chemometrics. *Molecules* **2022**, *27*, 4434. <https://doi.org/10.3390/molecules27144434>

Academic Editor: Tristan Richard

Received: 22 May 2022

Accepted: 29 June 2022

Published: 11 July 2022

Publisher’s Note: MDPI stays neutral with regard to jurisdictional claims in published maps and institutional affiliations.



Copyright: © 2022 by the authors. Licensee MDPI, Basel, Switzerland. This article is an open access article distributed under the terms and conditions of the Creative Commons Attribution (CC BY) license (<https://creativecommons.org/licenses/by/4.0/>).

1. Introduction

Low field time domain NMR (TD-NMR) relaxometry has great importance in food analyses due to its advantages, such as practicality, analytical productivity, rapid analysis, cost-effectiveness, and low-cost instrumentation [1–4]. Furthermore, since the applied radiofrequency (rf) is not attenuated by non-metallic materials (glass and plastic), TD-NMR analyses can be performed directly in the original packaging without requiring sample preparation nor generating waste [5,6].

The application of TD-NMR for food quality control in dairy products is one of its most widespread uses [7–9]. Some applications include detection and quantification of milk adulteration [10,11], determination of fat content in commercial products of milk powder [12], simultaneous quantification of fat and water content in cheese [13], characterization of yogurts [14], ice cream [15] and “requeijão cremoso” [16,17]. Requeijão cremoso (RC) is a type of processed cheese widely produced and consumed in Brazil [16,17]. It is prepared from the coagulation of pasteurized milk, with or without the addition of lactic cultures,

followed by the addition of cream, water, and melting salt (a mixture containing trisodium citrate) [17]. Studies investigated water mobility in the homemade RC with the addition of galactooligosaccharide (GOS) using TD-NMR relaxometry and showed an increase in the transversal relaxation time (T_2) with an increase of GOS [16]. Homemade RC with the addition of xylooligosaccharide (XOS), sodium reduction, and flavor enhancers (arginine and yeast extract) was also studied by TD-NMR relaxometry presented no differences in T_2 in the samples with 50% reduced salt content and with the addition of 1% of arginine or yeast extract [17]. However, a reduction in the T_2 values was observed in RC samples with lower fat content, which was associated with the decrease in mobility of water that strongly binds to the proteins. The addition of 3.3% of XOS also led to a substantial reduction in both transverse (T_2) and longitudinal (T_1) relaxation times.

The analysis of TD-NMR relaxometry of large samples, such as fresh fruits and oilseeds [18–20] and industrialized packaged food, can be performed using wide bore Halback, wide gap C and H types [21,22], or unilateral magnets [23,24]. The main advantage of Halback, C, or H types over the unilateral ones is the higher homogeneity of the magnetic field, allowing the analysis of the entire or large part of the sample. Conversely, unilateral magnets are cheaper and portable, and the magnet dimension does not limit the sample size. However, unilateral relaxometry has a strong magnetic field gradient, and only a small part of the sample is analyzed. Thus, the signal-to-noise ratio (SNR) in this equipment is very low and, consequently, the measuring time is much longer when compared to the developed in homogeneous magnets [21].

Most TD-NMR applications use the T_2 measurements [1,25]. These analyses are performed using Carr-Purcell-Meiboom-Gill (CPMG) pulse sequence, a single shot sequence that is very insensitive to the flip angle error and rf magnetic field inhomogeneity [21]. Applications based on the longitudinal (T_1) relaxation time are rarely used because the standard pulse sequences (inversion-recovery, saturation-recovery, progressive saturation, etc.) are not single shot sequences. Therefore, the measuring time is more than one order of magnitude longer than the CPMG measurement [21,26].

Another pulse sequence explored in the TD-NMR analysis is the continuous wave free precession (CWFP) [25,27,28], which is a special case of the steady-state free precession (SSFP) regime. In this sequence, rf pulses are separated by an interval shorter than the effective transverse relaxation time (T_2^*). When 90° pulses are used, CWFP signals depend on both T_1 and T_2 relaxation time. The first application of CWFP pulse sequence in low-field TD-NMR was proposed to enhance SNR to determine the hydrogen content in solvents and oil in seeds [21,25,27]. More recently, modifications in the CWFP pulse sequence were made, allowing to determine T_1 time in a fast and accurate way. The sequence was named CWFP- T_1 [27] and has been used in the analysis of packaged beef [29,30] and chicken breasts [31].

In this study, we demonstrated the viability of using CPMG and CWFP- T_1 to predict moisture, fat, and defatted dry mass content in RC commercial samples. To the best of our knowledge, it is the first time that a method based on TD-NMR has been proposed for RC quality control. Moreover, no paper was found in the literature reporting the use of TD-NMR to predict moisture, fat, and defatted dry mass content in dairy food samples directly in packaged commercial products. The analysis was performed using a TD-NMR spectrometer based on a wide bore Halback magnet and the data were analyzed using the partial least squares (PLS) regression method. This strategy represents a fast and promising analytical method for the dairy food chain.

2. Materials and Methods

2.1. Samples

This study comprised 45 commercial RC samples (27 traditional, 9 light, 4 vegan, 3 lactose-free, and 2 fibers) in plastic cups or tube packages, containing approximately 200 g of RC. The samples were obtained from a local market (São Carlos, SP, Brazil) and stored at 5 °C.

2.2. TD-NMR Measurements

The RC TD-NMR analyses were evaluated in a non-invasive and non-destructive way directly in the original packaging. ^1H TD-NMR experiments were evaluated using an SLK-IF-1399 NMR spectrometer (Spinlock Magnetic Resonance Solution, Cordoba, Argentine) equipped with a Halbach permanent magnet of 0.23 T (9 MHz for ^1H) and a 100 mm probe. Transverse relaxation time (T_2) measurements were performed using CPMG (Carr-Purcell-Meiboom-Gill) pulse sequence with a $\pi/2$ pulse width of 33 μs and π pulse width of 60 μs , echo time (τ) of 500 μs , 1000 echoes, and a recycle delay of 5 s. Values of longitudinal relaxation time (T_1) were determined using CWFP- T_1 (Continuous Wave Free Precession) pulse sequence [27] with a $\pi/2$ pulse width of 33 μs and $\pi/10$ pulse width of 4 μs , τ of 300 μs , 3000 echoes, and a recycle delay of 1 s. In both sequences, signals were averaged using 16 scans.

2.3. Chemical Analysis

The moisture content (grams of water per 100 g of RC product) was determined by drying the sample to a constant weight in an oven at 105 °C. Fat was determined gravimetrically after Soxhlet extraction of the dry matter (DM) using petroleum ether as extracting solvent. The extraction residue was considered the defatted dry mass (DDM). The fat content percentage was calculated in relation to dry (FDM) and wet matter (FWM), respectively.

2.4. Multivariate Analysis

The multivariate data analysis was performed using MATLAB R2021a (The Mathworks Inc., Natick, MA, USA) and PLS_Toolbox v.8.8 (Eigenvector Research Inc., Wenatchee, WA, USA).

The Principal Component Analysis (PCA) was used in a preliminary assessment to observe similarities and/or differences between the different types of RC samples. Before the analysis, the chemical data were auto-scaled and the TD-NMR decays (CPMG and CWFP- T_1) were mean-centered.

The multivariate calibration models were developed based on partial least squares (PLS) regression to quantify moisture, FDM, FWM, and DDM in RC samples. The Kennard–Stone algorithm divided the data into calibration (75% of the samples) and validation (25% of the samples) data sets. Before the analysis, the TD-NMR decays (CPMG and CWFP- T_1) were mean-centered. To improve the model reliability and develop simpler and predictive models, the algorithm ordered predictor selection (OPS) was used for variable selection. OPS Matlab routine can be freely obtained at <http://www.deq.ufv.br/chemometrics> [32].

The predictive ability of the final models was evaluated in terms of coefficient of determination (R^2), root mean square error of prediction (RMSEP), the relative error of prediction (REP), and ratio performance to deviation (RPD).

3. Results and Discussion

3.1. TD-NMR Decays

Figure 1 shows the TD-NMR signals of three RC samples with different chemical compositions acquired using CPMG (Figure 1a) and CWFP- T_1 (Figure 1b) pulse sequences. The TD-NMR relaxation curves are colored according to moisture content (black line = lowest, blue = medium, and red = highest moisture content). It is observed that the RC sample with the highest moisture (red line) had a significantly higher T_2 value than the sample with the lowest moisture content (black line). This is in agreement with results reported in the literature [33,34], which showed that an increase in moisture resulted in a higher T_2 relaxation time. Similar behavior was observed for T_1 values; The sample with the highest moisture (red line) had a significantly higher T_1 value than the sample with the lowest moisture (black line). T_2 and T_1 relaxation spectra of the three RC samples estimated by the Inverse Laplace transform (ILT) are shown respectively in Figure 1c,d [35]. The mean T_2 and T_1 relaxation curves show the presence of two populations, agreeing with previous studies in the literature, which reported that the T_2 relaxation in RC is mainly bi-exponential [16,17].

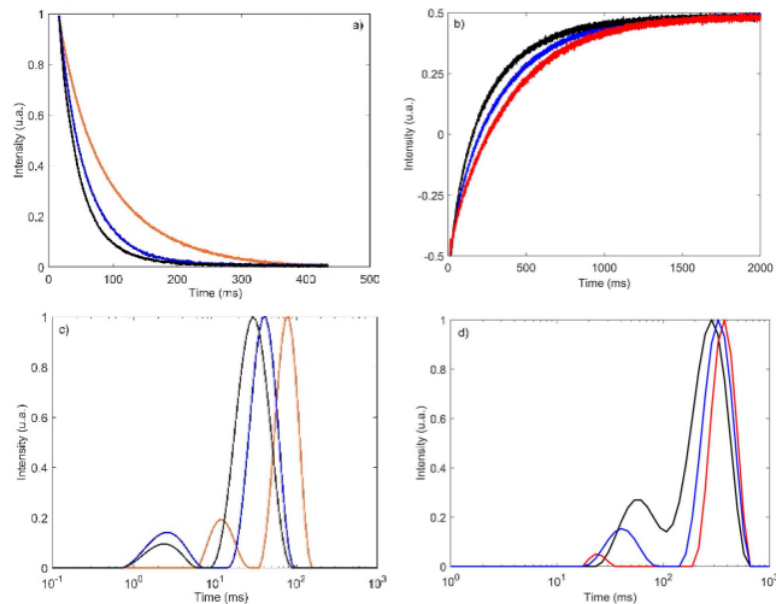


Figure 1. (a) CPMG and (b) CWFP- T_1 relaxation curves of three RC samples with different chemical compositions and the respective relaxation spectra (c,d) obtained with the ILT algorithm [35]. RC samples with the lowest, medium, and the highest moisture contents are the black, blue, and red lines, respectively.

The transverse relaxation times of the CPMG curves (Figure 1a) showed that the samples with low, medium, and high moisture could be resolved into a fast-relaxing time constant (T_{21}) equals to 2, 3, and 12 ms, respectively, and a slow-relaxing time constant (T_{22}) equals to 30, 41, and 78 ms, respectively. For CWFP- T_1 signals, the RC samples with low, medium, and high moisture showed T_{11} values of 23, 43, and 58 ms, respectively, and a T_{12} of 329, 374, and 284 ms, respectively.

As RC contains between 55 and 80% of water and less than 22% of fat, the relaxation signals are dominated by the water relaxation time. As $T_1 > T_2$ is an indication that water mobility is restricted by the interaction of dry matter products, mainly lipids, proteins, and saccharides that correspond to 20–45% of the RC.

3.2. Exploratory Analysis

Preliminary data exploration with the PCA was performed in the chemical results (moisture, FDM, FWM, and DDM) to investigate natural differences and patterns among samples and highlight relationships between variables and classes. For this proposed, 45 commercially available RC samples composed of 27 traditional, 9 light, 4 vegan, 3 lactose-free, and 2 fibers, were disposed of in a matrix X (45×4). The results are presented on the PCA biplot (Figure 2). The first two principal components (PC1 and PC2) explained 99.8% of the total variance (81.2% and 18.6%, respectively) and provided a slight separation of traditional and vegan samples from the other RC types (light, lactose-free, and fiber). The examination of loadings revealed that the variables that most contributed to this separation were FWM and FDM, which are positioned positively on PC1. These results are in agreement with the chemical values, which revealed that the traditional and vegan samples had the highest fat content in dry ($61.4 \pm 9.3\%$ and $67.4 \pm 3.1\%$, respectively) and wet ($23.2 \pm 4.6\%$ and $28.1 \pm 1.7\%$, respectively) matter. Conversely, moisture and defatted dry mass are directly correlated with light, fiber, and lactose-free samples, since they are positioned negatively on PC1. The chemical results revealed that these samples showed the highest moisture values, ranging from 60.6 to 77.4%, and defatted dry mass, ranging from 11.1 to 20.1%.

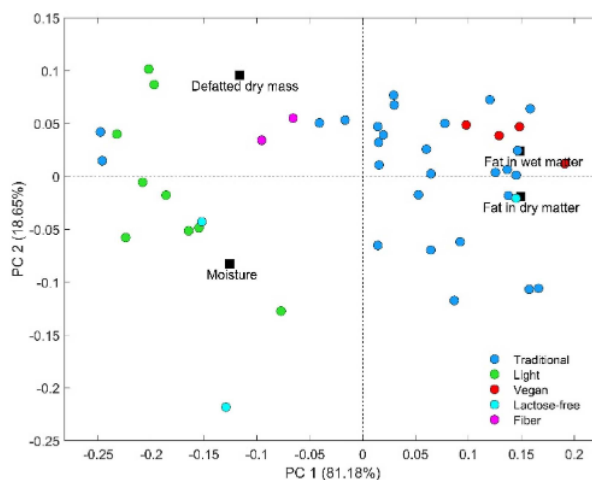


Figure 2. Scores (circles) and loadings (squares) biplot of the first two components of a PCA model of the RC samples.

CPMG and CWFP- T_1 decays of the 45 samples were also analyzed by the PCA. Inspection of the PCA subspaces (bi- or three-dimensional score plot) did not reveal groups of samples with respect to the RC type (data not shown). These results suggest no significant differences in T_2 and T_1 time decay profiles were observed among the samples. However, due to the limited number of commercial samples, it was not possible to confirm that the method cannot be applied to distinguish the RC samples.

3.3. Regression Models

Initial PLS models were built by correlating the full TD-NMR decay and reference values of moisture, FDM, FWM, and DDM. As already mentioned (Section 2.4), the whole data set (27 traditional, 9 light, 4 vegan, 3 lactose-free, and 2 fibers) was divided into 33 samples for the training set and 12 samples for the test set. The models were optimized through the detection of outliers based on samples with extreme leverages, large residuals in the X block (spectral outliers) or in the Y block (prediction outliers) were detected at the 95% confidence level. The number of latent variables (LV) was chosen based on the smallest RMSECV values estimated using random subsets (10 data splits and 20 iterations). The figures of merit of the models showed that the predictions were not very accurate and thus could not be considered satisfactory. To confirm the model significance, a permutation test was performed, in which 100 interactions were performed comparing permuted with unpermuted models considering self-prediction and cross-validation. The Wilcoxon signed-rank test (Wilcoxon) indicates that the models are significant at a 95% confidence level. Moreover, in the self-prediction approach, the signed-rank test (sign test) and randomization t -test (Rand t test) were above 0.05, indicating that these models (permuted and nonpermuted) are not significantly different at the 95% limit. Since this outcome could be attributed to the possible presence of a high amount of irrelevant and/or noisy variables in the data set, the OPS variable selection was conducted.

The comparison of the PLS models with and without variable reduction for DDM quantification is shown in Table 1. The best models were obtained autoOPS algorithm, with a window of 10 and increments of 5, which is coherent with the literature [32]. The number of variables used to build the models was significantly reduced from 993 to 205 for CPMG data and from 5965 to 75 for CWFP- T_1 data [36]. The models were obtained with 3 LV, providing parsimonious models. It can be seen that the variable selection steps increase the accuracy of the CWFP- T_1 model. Comparing the results obtained with “full data”, the OPS-PLS model attained the best results with an RMSEP value of 1.38% and R^2_{pred} of 0.90. Conversely, results suggested that the variable selection did not significantly improve the CPMG model in terms of RMSEP, RPD, and REP. A permutation test indicated

that both OPS-PLS models were substantially different from the unpermuted ones and did not display overfitting at a 95% level.

Table 1. Performance parameters of the PLS models obtained using all variables and those selected by the OPS algorithm for DDM quantification.

	CPMG		CWFP	
	Full	OPS	Full	OPS
Nvars *	993	205	5965	75
LV	3	3	3	3
RMSEP **	1.51	1.53	1.84	1.38
R^2_{pred}	0.49	0.67	0.82	0.90
RPD _{pred}	1.37	1.36	1.46	1.95
REP _{pred} **	9.55	9.67	11.60	8.70

* number of variables. ** % w w⁻¹.

The RPD value can also confirm the good prediction capacity of the CWFP-T₁ model. RPD is a dimensionless figure of merit specifically used to evaluate the trueness of multivariate calibration models in absolute terms. According to the literature [37–39], desirable calibration models must have an RPD higher than 2.4, while RPD values between 2.4 and 1.5 are considered acceptable. Models with RPD less than 1.5 are considered unusable. Thus, the RPD value for the CWFP-T₁ model was considered satisfactory, whereas the RPD value for the CPMG model was considered unusable. The REP was another figure of merit calculated to evaluate the trueness of the models, whose values were 9.55 and 8.70% w w⁻¹, for the CPMG and CWFP-T₁ models, respectively. This scenario is completely acceptable once the analysis was performed directly on the packaged commercial products. These results can also be graphically visualized in Figure 3, where the measured vs. predicted plots for both the calibration and validation sets are displayed.

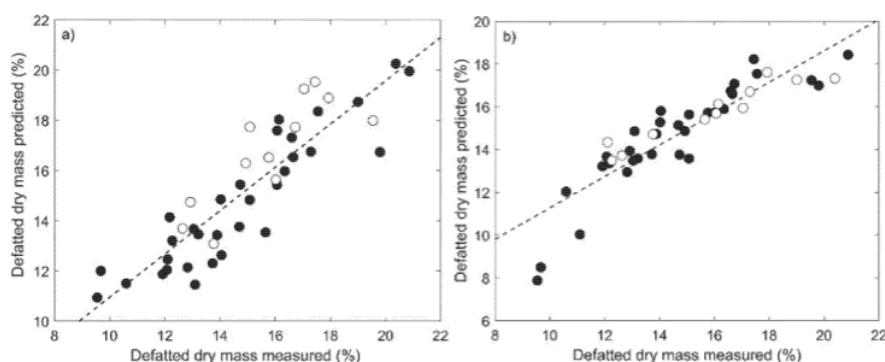


Figure 3. Plots of reference versus predicted values for the calibration (black circles) and validation (white circles) samples for (a) CPMG and (b) CWFP-T₁.

Similar approaches were explored to quantify FWM, FDM, and moisture in the RC samples. The commercial samples presented FWM contents from 33 to 73% w w⁻¹, FDM contents from 9 to 30% w w⁻¹, and moisture contents from 56 to 77% w w⁻¹. The PLS models were developed using the autoOPS algorithm, with a window of 10 and increments of 5. The number of variables used to build the models was 205 and 75 for CPMG and CWFP-T₁, respectively. The best models were obtained with 4 LV. Results showed that the CPMG models are inadequate to predict fat in wet and dry matter and moisture in the RC samples, with lower values of R^2_{pred} (<0.28) and RPD_{pred} (<1.26) and higher values of RMSEP and REP (>7.71 w w⁻¹) (Table 2). Furthermore, a permutation test indicated that models were not significantly different from the unpermuted ones at the 95% level. Conversely, the models developed using CWFP-T₁ data showed to be suitable with R^2_{pred}

of 0.92, RMSEP of 4.71% w w⁻¹, REP of 8.79% w w⁻¹ and RPD_{pred} of 2.92 for fat in wet matter, R²_{pred} of 0.85, RMSEP of 3.28% w w⁻¹, RPD_{pred} of 16.68% w w⁻¹ and RPD_{pred} of 2.32 for fat in wet matter the model and R²_{pred} of 0.70, RMSEP of 3.00% w w⁻¹, REP of 4.65% w w⁻¹ and RPD_{pred} of 1.77 for moisture.

Table 2. PLS models obtained for FDM, FWM, and moisture quantification using the OPS algorithm.

	CPMG			CWFP-T ₁		
	Fat in Dry Matter	Fat in Wet Matter	Moisture	Fat in Dry Matter	Fat in Wet Matter	Moisture
RMSEP *	10.90	6.12	4.97	4.71	3.28	3.00
R ² _{pred}	0.28	0.23	0.050	0.92	0.85	0.70
RPD _{pred}	1.26	1.24	1.07	2.92	2.32	1.77
REP _{pred} *	20.35	31.13	7.71	8.79	16.68	4.65

* % w w⁻¹.

The reference vs. predicted values for (a) FWM (% w w⁻¹), (b) FDM (% w w⁻¹) and (c) moisture content (% w w⁻¹) by using CWFP-T₁ decays combined with the OPS selection variable method are shown in Figure 4.

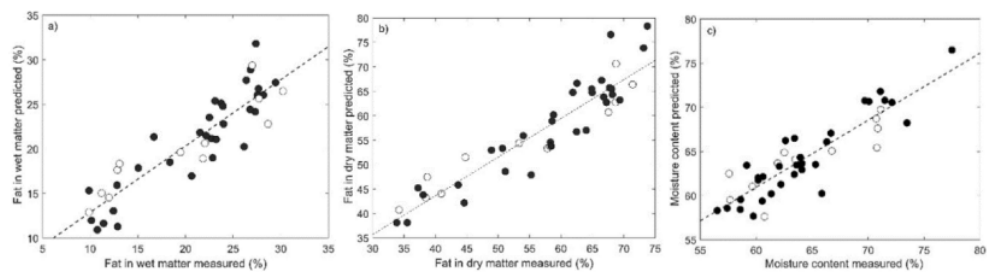


Figure 4. Plots of the reference versus predicted values for the calibration (black circles) and validation (white circles) samples for (a) FWM, (b) FDM, and (c) moisture obtained with CWFP-T₁ data.

Regression models were also evaluated by correlating the T₁ or T₂ values against the moisture, fat, and defatted dry matter contents (univariate approaches) and combining T₁ and T₂ values (multivariate approaches). However, results obtained with the full TD-NMR decays showed better predictability, with a higher correlation coefficient. Therefore, only these results were shown in detail in the manuscript.

Methods based on near- and mid-infrared spectroscopy have been reported in the literature for moisture and fat determination in dairy products, especially in cheese [40]. Nevertheless, no study on RC samples was found. A procedure to quantify fat and moisture in cow mozzarella cheeses by using reflectance near-infrared spectroscopy has been developed and validated [37]. The PLS models were constructed within the ranges from 38.7 to 58.0% w w⁻¹ on dry basis for fat and from 41.5 to 55.1% w w⁻¹ for moisture, providing RMSEP of 2.1 and 0.9%, respectively. The performance of near- and mid-infrared spectroscopy to determine several quality parameters of cheese, including moisture and fat was compared [41] and the results showed that near-infrared spectroscopy was more accurate than mid-infrared, with RPD of 2.14 and 3.38% for fat and moisture, respectively [41]. These infrared procedures showed better predictability than the results acquired with TD-NMR. However, the proposed TD-NMR relaxometry method is interesting because it is applicable in through-package determinations, which is not possible with the infrared ones. Thus, the RC parameters can be predicted using TD-NMR relaxometry and chemometrics without violating the seal of packages.

4. Conclusions

Wide bore low field time domain NMR (TD-NMR) relaxometry data, modeled by chemometrics methods, can be a fast and non-invasive procedure to predict fat, defatted dry mass, and moisture content in RC samples. The models were developed using 45 commercially available RC samples (27 traditional, 9 light, 4 vegan, 3 lactose-free, and 2 fibers). The PLS models obtained with T_1 relaxation time measured with a single shot CWFP- T_1 pulse showed better predictability than the models evaluated with T_2 relaxation time measured with the CPMG pulse sequence. In addition, the PLS model performances were improved when combined with OPS variable selection method. Therefore, CWFP- T_1 data modeled with chemometrics can be a fast method to monitor the quality of RC directly in commercial packages. However, the potential of CWFP- T_1 sequence in TD-NMR spectrometer still needs to be verified with a larger number of RC samples to obtain a robust regression model to predict fat, moisture, and defatted dry matter.

Author Contributions: G.d.O.M.: NMR and chemical measurements. G.G.T.: Data curation, Formal analysis, Investigation, Methodology, Validation, Visualization. R.H.d.S.G.: NMR measurements and processing. T.B.M.: inverse Laplace analyses, writing—original-draft preparation. E.B.: Data curation, Formal analysis, Validation, Visualization, Methodology, Writing—original draft. P.M.S.: Data curation, Formal analysis, Validation, Visualization, Writing—review & editing. L.A.C.: Conceptualization, Funding acquisition, Project administration, Resources, Supervision, Validation, Visualization, Writing—review & editing. All authors have read and agreed to the published version of the manuscript.

Funding: This research was funded by Brazilian Agencies FAPESP grant 2021/12694-3 and CNPq, grant 307635/2021-0 and 409111/2016-3.

Data Availability Statement: The data presented in this study are available on request from the corresponding author.

Conflicts of Interest: The authors declare no conflict of interest.

Sample Availability: Samples of the compounds are not available from the authors.

References

1. Ezeanaka, M.C.; Nsor-Atindana, J.; Zhang, M. Online Low-field Nuclear Magnetic Resonance (LF-NMR) and Magnetic Resonance Imaging (MRI) for Food Quality Optimization in Food Processing. *Food Bioprocess Technol.* **2019**, *12*, 1435–1451. [[CrossRef](#)]
2. van Duynhoven, J.; Voda, A.; Witek, M.; Van As, H. Chapter 3—Time-Domain NMR Applied to Food Products. In *Annual Reports on NMR Spectroscopy*; Webb, G.A., Ed.; Academic Press: Cambridge, MA, USA, 2010; Volume 69, pp. 145–197.
3. Kirtil, E.; Oztop, M.H. H-1 Nuclear Magnetic Resonance Relaxometry and Magnetic Resonance Imaging and Applications in Food Science and Processing. *Food Eng. Rev.* **2016**, *8*, 1–22. [[CrossRef](#)]
4. Pearce, K.L.; Rosenvold, K.; Andersen, H.J.; Hopkins, D.L. Water distribution and mobility in meat during the conversion of muscle to meat and ageing and the impacts on fresh meat quality attributes—A review. *Meat Sci.* **2011**, *89*, 111–124. [[CrossRef](#)] [[PubMed](#)]
5. Pereira, F.M.V.; Rebellato, A.P.; Pallone, J.A.L.; Colnago, L.A. Through-package fat determination in commercial Samples of mayonnaise and salad dressing using time-domain nuclear magnetic resonance spectroscopy and chemometrics. *Food Control* **2015**, *48*, 62–66. [[CrossRef](#)]
6. Santos, P.M.; Kock, F.V.C.; Santos, M.S.; Lobo, C.M.S.; Carvalho, A.S.; Colnago, L.A. Non-Invasive Detection of Adulterated Olive Oil in Full Bottles Using Time-Domain NMR Relaxometry. *J. Braz. Chem. Soc.* **2017**, *28*, 385–390. [[CrossRef](#)]
7. Maher, A.D.; Rochfort, S.J. Applications of NMR in Dairy Research. *Metabolites* **2014**, *4*, 131–141. [[CrossRef](#)]
8. Poca, P.; Mecit Halil, O. Chapter 10—Low-field time-domain nuclear magnetic resonance applied to dairy foods. In *Dairy Foods*; da Cruz, A.G., Ranadheera, C.S., Nazzaro, F., Mortazavian, A.M., Eds.; Woodhead Publishing: Duxford, UK, 2022; pp. 215–232.
9. Mariette, F. NMR Relaxation of Dairy Products. In *Modern Magnetic Resonance*; Webb, G.A., Ed.; Springer: Dordrecht, The Netherlands, 2006; Volume 1, pp. 1697–1701.
10. Pablo, T.C.; Bathazar, C.F.; Guimarães, J.T.; Coutinho, N.M.; Pimentel, T.C.; Neto, R.P.C.; Esmerino, E.A.; Freitas, M.Q.; Silva, M.C.; Tavares, M.I.B.; et al. Detection of formaldehyde in raw milk by time domain nuclear magnetic resonance and chemometrics. *Food Control* **2020**, *110*, 107006. [[CrossRef](#)]
11. Santos, P.M.; Pereira-Filho, E.R.; Colnago, L.A. Detection and quantification of milk adulteration using time domain nuclear magnetic resonance (TD-NMR). *Microchem. J.* **2016**, *124*, 15–19. [[CrossRef](#)]

12. Nascimento, P.A.M.; Barsanelli, P.L.; Rebellato, A.P.; Pallone, J.A.L.; Colnago, L.A.; Pereira, F.M.V. Time-Domain Nuclear Magnetic Resonance (TD-NMR) and Chemometrics for Determination of Fat Content in Commercial Products of Milk Powder. *J. AOAC Int.* **2017**, *100*, 330–334. [[CrossRef](#)]
13. Castell-Palou, A.; Rossello, C.; Femenia, A.; Simal, S. Simultaneous Quantification of Fat and Water Content in Cheese by TD-NMR. *Food Bioprocess Technol.* **2013**, *6*, 2685–2694. [[CrossRef](#)]
14. Yu, H.-Y.; Wang, L.; Kathryn, L.M. Characterization of yogurts made with milk solids nonfat by rheological behavior and nuclear magnetic resonance spectroscopy. *J. Food Drug Anal.* **2016**, *24*, 804–812. [[CrossRef](#)] [[PubMed](#)]
15. Lucas, T.; Wagener, M.; Barey, P.; Mariette, F. NMR assessment of mix and ice cream. Effect of formulation on liquid water and ice. *Int. Dairy J.* **2005**, *15*, 1064–1073. [[CrossRef](#)]
16. Belsito, P.C.; Ferreira, M.V.S.; Cappato, L.P.; Cavalcanti, R.N.; Vidal, V.A.S.; Pimentel, T.C.; Esmerino, E.A.; Balthazar, C.F.; Neto, R.P.C.; Tavares, M.I.B.; et al. Manufacture of Requeijao cremoso processed cheese with galactooligosaccharide. *Carbohydr. Polym.* **2017**, *174*, 869–875. [[CrossRef](#)]
17. Ferrao, L.L.; Ferreira, M.V.S.; Cavalcanti, R.N.; Carvalho, A.F.A.; Pimentel, T.C.; Silva, H.L.A.; Silva, R.; Esmerino, E.A.; Neto, R.P.C.; Tavares, M.I.B.; et al. The xylooligosaccharide addition and sodium reduction in requeijao cremoso processed cheese. *Food Res. Int.* **2018**, *107*, 137–147. [[CrossRef](#)] [[PubMed](#)]
18. de Andrade, F.D.; Netto, A.M.; Colnago, L.A. Qualitative analysis by online nuclear magnetic resonance using Carr-Purcell-Meiboom-Gill sequence with low refocusing flip angles. *Talanta* **2011**, *84*, 84–88. [[CrossRef](#)] [[PubMed](#)]
19. Pereira, F.M.V.; Carvalho, A.D.; Cabeca, L.F.; Colnago, L.A. Classification of intact fresh plums according to sweetness using time-domain nuclear magnetic resonance and chemometrics. *Microchem. J.* **2013**, *108*, 14–17. [[CrossRef](#)]
20. Bizzani, M.; Flores, D.W.M.; Moraes, T.B.; Colnago, L.A.; Ferreira, M.D.; Spoto, M.H.F. Non-invasive detection of internal flesh breakdown in intact Palmer mangoes using time-domain nuclear magnetic resonance relaxometry. *Microchem. J.* **2020**, *158*, 105208. [[CrossRef](#)]
21. Moraes, T.B.; Colnago, L.A. Noninvasive Analyses of Food Products Using Low-field Time-domain NMR: A Review of Relaxometry Methods. *Braz. J. Phys.* **2022**, *52*. [[CrossRef](#)]
22. Parker, A.J.; Zia, W.; Rehorn, C.W.G.; Blumich, B. Shimming Halbach magnets utilizing genetic algorithms to profit from material imperfections. *J. Magn. Reson.* **2016**, *265*, 83–89. [[CrossRef](#)]
23. Pedersen, H.T.; Ablett, S.; Martin, D.R.; Mallett, M.J.D.; Engelsen, S.B. Application of the NMR-MOUSE to food emulsions. *J. Magn. Reson.* **2003**, *165*, 49–58. [[CrossRef](#)]
24. Blumich, B.; Blumler, P.; Eidmann, G.; Guthausen, A.; Haken, R.; Schmitz, U.; Saito, K.; Zimmer, G. The NMR-mouse: Construction, excitation, and applications. *Magn. Reson. Imaging* **1998**, *16*, 479–484. [[CrossRef](#)]
25. Monaretto, T.; Moraes, T.B.; Colnago, L.A. Recent 1D and 2D TD-NMR Pulse Sequences for Plant Science. *Plants* **2021**, *10*, 833. [[CrossRef](#)]
26. Blumich, B. Introduction to compact NMR: A review of methods. *Trac-Trends Anal. Chem.* **2016**, *83*, 2–11. [[CrossRef](#)]
27. Moraes, T.B.; Monaretto, T.; Colnago, L.A. Rapid and simple determination of T-1 relaxation times in time-domain NMR by Continuous Wave Free Precession sequence. *J. Magn. Reson.* **2016**, *270*, 1–6. [[CrossRef](#)] [[PubMed](#)]
28. Moraes, T.B.; Monaretto, T.; Colnago, L.A. Applications of Continuous Wave Free Precession Sequences in Low-Field, Time-Domain NMR. *Appl. Sci.* **2019**, *9*, 1312. [[CrossRef](#)]
29. Cônsolo, N.R.B.; Silva, J.; Buarque, V.L.M.; Samuelsson, L.M.; Miller, P.; Maclean, P.H.; Moraes, T.B.; Barbosa, L.C.G.S.; Higuera-Padilla, A.; Colnago, L.A.; et al. Using TD-NMR relaxometry and 1D ¹H NMR spectroscopy to evaluate aging of Nellore beef. *Meat Sci.* **2021**, *181*, 108606. [[CrossRef](#)]
30. Monaretto, T.; Montrazi, E.T.; Moraes, T.B.; Souza, A.A.; Rondeau-Mouro, C.; Colnago, L.A. Using T-1 as a direct detection dimension in two-dimensional time-domain NMR experiments using CWFP regime. *J. Magn. Reson.* **2020**, *311*. [[CrossRef](#)]
31. Consolo, N.R.B.; Samuelsson, L.M.; Barbosa, L.; Monaretto, T.; Moraes, T.B.; Buarque, V.L.M.; Higuera-Padilla, A.R.; Colnago, L.A.; Silva, S.L.; Reis, M.M.; et al. Characterization of chicken muscle disorders through metabolomics, pathway analysis, and water relaxometry: A pilot study. *Poult. Sci.* **2020**, *99*, 6247–6257. [[CrossRef](#)] [[PubMed](#)]
32. Roque, J.V.; Cardoso, W.; Peternelli, L.A.; Teofilo, R.F. Comprehensive new approaches for variable selection using ordered predictors selection. *Anal. Chim. Acta* **2019**, *1075*, 57–70. [[CrossRef](#)] [[PubMed](#)]
33. Hansen, C.L.; Thybo, A.K.; Bertram, H.C.; Viereck, N.; van den Erg, F.; Engelsen, S.B. Determination of Dry Matter Content in Potato Tubers by Low-Field Nuclear Magnetic Resonance (LF-NMR). *J. Agric. Food Chem.* **2010**, *58*, 10300–10304. [[CrossRef](#)]
34. Jepsen, S.M.; Pedersen, H.T.; Engelsen, S.B. Application of chemometrics to low-field H-1 NMR relaxation data of intact fish flesh. *J. Sci. Food Agric.* **1999**, *79*, 1793–1802. [[CrossRef](#)]
35. Moraes, T.B. Transformada Inversa de Laplace para análise de sinais de Ressonância Magnética Nuclear de Baixo Campo. *Química Nova* **2021**, *44*, 7. [[CrossRef](#)]
36. Monaretto, T.; Souza, A.; Moraes, T.B.; Bertucci-Neto, V.; Rondeau-Mouro, C.; Colnago, L.A. Enhancing signal-to-noise ratio and resolution in low-field NMR relaxation measurements using post-acquisition digital filters. *Magn. Reson. Chem.* **2019**, *57*, 616–625. [[CrossRef](#)] [[PubMed](#)]
37. Botelho, B.G.; Mendes, B.A.P.; Sena, M.M. Development and Analytical Validation of Robust Near-Infrared Multivariate Calibration Models for the Quality Inspection Control of Mozzarella Cheese. *Food Anal. Methods* **2013**, *6*, 881–891. [[CrossRef](#)]

38. Olarewaju, O.O.; Magwaza, L.S.; Nieuwoudt, H.; Poblete-Echeverria, C.; Fawole, O.A.; Tesfay, S.Z.; Opara, U.L. Model development for non-destructive determination of rind biochemical properties of 'Marsh' grapefruit using visible to near-infrared spectroscopy and chemometrics. *Spectrochim. Acta Part A-Mol. Biomol. Spectrosc.* **2019**, *209*, 62–69. [[CrossRef](#)]
39. Aleixandre-Tudo, J.L.; Nieuwoudt, H.; Olivieri, A.; Aleixandre, J.L.; du Toit, W. Phenolic profiling of grapes, fermenting samples and wines using UV-Visible spectroscopy with chemometrics. *Food Control* **2018**, *85*, 11–22. [[CrossRef](#)]
40. Bittante, G.; Patel, N.; Cecchinato, A.; Paolo, B. Invited review: A comprehensive review of visible and near-infrared spectroscopy for predicting the chemical composition of cheese. *J. Dairy Sci.* **2022**, *105*, 1817–1836. [[CrossRef](#)]
41. Ayvaz, H.; Mortas, M.; Dogan, M.A.; Atan, M.; Tiryaki, G.Y.; Yuceer, Y.K. Near- and mid-infrared determination of some quality parameters of cheese manufactured from the mixture of different milk species. *J. Food Sci. Technol.* **2021**, *58*, 3981–3992. [[CrossRef](#)]